Available online at www.sciencedirect.com
SCIENCE DIRECT
Biochemical and Biophysical Research Communications 343 (2006) 190–197
BBRC
www.elsevier.com/locate/ybbrc

rAAV-mediated shRNA ameliorated neuropathology in Huntington disease model mouse

Yoko Machida [a], Takashi Okada [b], Masaru Kurosawa [a], Fumitaka Oyama [a], Keiya Ozawa [b], Nobuyuki Nukina [a,*]

[a] *Laboratory for Structural Neuropathology, RIKEN Brain Science Institute, 2-1 Hirosawa, Wako-shi, Saitama 351-0198, Japan*
[b] *Division of Genetic Therapeutics, Center for Molecular Medicine, Jichi Medical School, 3311-1 Yakushiji, Minami-Kawachi, Tochigi 329-0498, Japan*

Received 21 February 2006
Available online 3 March 2006

Abstract

Huntington disease (HD) is a fatal progressive neurodegenerative disorder associated with expansion of a CAG repeat in the first exon of the gene coding the protein huntingtin (htt). Although the feasibility of RNA interference (RNAi)-mediated reduction of htt expression to attenuate HD-associated symptoms is suggested, the effects of post-symptomatic RNAi treatment in the HD model mice have not yet been certified. Here we show the effects of recombinant adeno-associated virus (rAAV)-mediated delivery of RNAi into the HD model mouse striatum after the onset of disease. Neuropathological abnormalities associated with HD, such as insoluble protein accumulation and down-regulation of DARPP-32 expression, were successfully ameliorated by the RNAi transduction. Importantly, neuronal aggregates in the striatum were reduced after RNAi transduction in the animals comparing to those at the time point of RNAi transduction. These results suggest that the direct inhibition of mutant gene expression by rAVV would be promising for post-symptomatic HD therapy.

Keywords: Polyglutamine; Huntington disease; DARPP-32; Adeno-associated virus; RNAi

Huntington disease (HD) is an autosomal dominant neurodegenerative disorder, characterized by cognitive abnormalities and involuntary movements. Selective loss of brain neurons and the formation of intranuclear aggregates were observed [1]. HD is resulting from polyglutamine repeat (CAG repeat: polyQ) expansion in the protein huntingtin (htt). Expanded polyQ alters the protein conformation and then recruits many essential proteins such as transcription-regulating proteins, molecular chaperones, and ubiquitin-binding proteins [2–6]. Mutant htt also impairs the function of the ubiquitin-proteasome system [4,7] and also induces mitochondrial calcium defects [8].

For therapeutic treatment of HD, several substances, such as Congo red and trehalose, have beneficial effects to inhibit oligomerization or stabilize polyQ bearing molecules [9,10]. These approaches targeted downstream of mutant protein expression. In contrast, gene silencing by RNA interference (RNAi) targets mRNA of mutant protein in a sequence-specific manner and reduces mutant protein expression [11]. Introduction of 21-nt short interfering RNAs (siRNAs) into mammalian cells effectively inhibits endogenous genes without a non-specific viral response. Vector-based synthesis of siRNAs became available to use in various cells and tissues [12–14]. Taking advantage of this approach, gene silencing of mutant mRNA through RNAi provides a direct approach in the treatment of neurodegenerative diseases. Lentiviral vector-mediated delivery of short hairpin siRNAs (shRNAs) targeting SOD1 (superoxide dismutase 1) to the SOD1 mutant mouse resulted in the delayed onset, improvement of behavioral defects, and protection from neuronal degeneration in the spinal cord [15]. shRNAs targeting ataxin-1 were also delivered to the cerebellum by recombinant adeno-associated virus (rAAV) to improve pathological abnormalities, reduc-

* Corresponding author. Fax: +81 48 462 4796.
E-mail address: nukina@brain.riken.jp (N. Nukina).

0006-291X/$ - see front matter © 2006 Elsevier Inc. All rights reserved.
doi:10.1016/j.bbrc.2006.02.141

ing the intranuclear inclusions and restoring the cerebellar morphology [16]. In HD, many studies have suggested toxic gain-of-function by mutant htt plays a role, thus a gene silence strategy is likely a promising therapy for HD. More recently, injection of vector-based shRNA against huntingtin improved motor disturbance and neuropathological abnormalities [17,18]. Furthermore, introduction of synthesized siRNA against htt delayed disease onset with the improvement of motor disturbance, neuropathological abnormalities, and longevity in the HD model mouse [15,19]. However, these RNAi treatments were provided at the early pre-symptomatic stage of neurodegenerative disorder in each transgenic model.

Previously, a conditional model of HD using a tetracycline-regulation system showed that mice expressing a mutated htt fragment demonstrated neuronal inclusions and progressive motor dysfunction [20]. In this model, blocking expression in symptomatic mice led to the disappearance of inclusions and amelioration of the behavioral phenotype. Thus, reduction of htt expression by RNAi may attenuate HD-associated symptom progression even if treatment is carried out after the onset of symptoms. In this study, taking advantage of truncated htt-EGFP transgenic mouse in which the aggregates are visualized by EGFP fluorescence, we investigated the neuropathological changes in HD model mice by suppression of transgene with shRNAs delivered by rAAV.

Materials and methods

HD model mouse. The HD190QG transgenic mouse was used as a HD model in this study. The HD190QG transgenic mouse harbors mutant truncated N-terminal htt containing 190 CAG repeats fused with EGFP in its genome. This animal shows progressive motor abnormality, and neuropathology such as formation of aggregates in brain, and shorter viability [21]. All the experiments with mice were approved by the Animal Experiment Committee of the RIKEN Brain Science Institute.

Construction and production of rAAV. Ten candidate sequences for short hairpin RNAs targeting EGFP mRNA were ligated into a pSilencer A plasmid (Ambion, Inc., Austin, TX). Neuro2a cells were co-transfected with each shRNA in pSilencer and EGFP expression vector pEGFP-N1 (BD Biosciences Clontech, Palo Alto, CA). The effect of gene silencing was evaluated by Western blot analysis using GFP antibody (Roche Molecular Biochemicals, Indianapolis, IN) to choose an effective sequence of shRNA (shEGFP) and non-effective sequence as a control (shEGFPcontrol). The shEGFP expression cassette containing U6 promoter was obtained by PCR with primers containing a *Hin*d III restriction site, forward primer: 5′-CCCAAGCTTGGGATCTTACCGCTGTTGAGA-3′ and reverse primer: 5′-CCCAAGCTTGGGCCACACTTCAAGAACTC-3′. The monomeric red fluorescence protein (mRFP) cDNA was derived from mRFP1 in $pRSET_B$ [22] and ligated into pcDNA3 (Invitrogen Corporation, Carlsbad, CA). The shEGFP expression cassette was ligated into a proviral vector plasmid bearing inverted terminal repeats derived from AAV2 or AAV5 (pAAV-LacZ or pAAV5-RNL) to create pAAV2-shEGFP or pAAV5-shEGFP. mRFP expression cassette driven by CMV promoter was also inserted into the vector plasmid to visualize transduction (Fig. 1A). rAAV-shEGFP and rAAV-shEGFPcontrol were prepared according to three-plasmid transfection protocol described previously [23,24]. The viral stock was titrated by dot-blot hybridization with plasmid standards to make a stock of 1×10^{10} genome copies/μl.

In vitro assay of shRNA effect. HEK 293 cells was transfected with the pEGFP-N1 or plasmids expressing N-terminal htt exon 1 gene containing 16, 60, and 150 CAG repeats fused with EGFP (Nhtt16QG, Nhtt60QG, and Nhtt150QG, respectively). Four hours after transfection, rAAV2-shEGFP or shEGFPcontrol was added to the culture medium at 1×10^5 genome copies/cell. The EGFP fluorescence intensity was analyzed by the Cellomics™ Array Scan®V™ System (Beckman Coulter Inc., Fullerton, CA) after 48 h of viral transduction. The relative level of GFP intensity within the RFP-positive area transduced with rAAV-shEGFP or rAAV-shEGFPcontrol was estimated.

Virus injection into the mouse brain. Virus injection was performed by using the following coordinates with respect to the bregma; 0.5 mm anterior, 2 mm lateral, 3 mm depth, 0.3 μl/min infusion rate, and 3 μl per site. An equal amount of buffer was simultaneously injected into the contralateral side of the brain. The viral injection was carried out at the age of 8 weeks or 12 weeks, and analysis was performed at the age of 24 weeks.

Detection of virus transduction and aggregates by fluorescent imager. Mouse brains were perfused and fixed overnight with 4% paraformaldehyde. Serial-cut 40-micrometer sections were analyzed with a laser-scanning imaging system (Molecular Imager FX; Bio-Rad Laboratories, Hercules, CA) with an external laser (Bio-Rad Laboratories). Sections were imaged using the 488-nm laser with the standard 530 bandpass emission filter for detection of GFP fluorescence and 532-nm laser with the standard 640 nm bandpass emission filter for detection of RFP fluorescence as described previously [21].

Immunohistochemistry and aggregate count. Serial-cut 40-micrometer free-floating sections were used for immunohistochemistry. Sections were treated with anti-RFP antibody (Clontech) followed by AlexaFluor 568-labeled anti-rabbit secondary antibody (Molecular Probes). Aggregates were counted using images of immunohistochemistry with antibodies against EGFP (Nacalai Tesque, Inc., Kyoto, Japan), htt (Chemicon International, Inc., Temecula, CA), and ubiquitin (Dako, Glostrup, Denmark) followed by detection using ABC Elite kit (Vector Laboratories, Inc., Burlingame, CA). The number of aggregates was calculated using MacSCOPE (Mitani, Tokyo, Japan) after normalizing the contrast and brightness of the digital images as described previously [10].

Filter trap assay. The striatum, cortex, and hippocampus were sampled and homogenated in 5 volumes of IMAC buffer (20 mM Hepes, pH 7.4, 140 mM potassium acetate, 1 mM magnesium acetate, and 1 mM EGTA with EDTA-free complete protease inhibitor cocktail tablets; Roche) with seven strokes using the digital homogenizer (As One, Osaka, Japan) at 1000 rpm. Homogenate containing 10 μg of protein was diluted with 0.2 ml of 2% SDS and filtered through a 0.2 μm cellulose acetate membrane (Advantec Toyo Roshi Kaisha Ltd., Tokyo Japan). Captured insoluble protein was detected by incubation with antibodies against GFP (Roche) and htt (Chemicon) followed by incubation with secondary antibodies and fluorescence substrates. Insoluble protein was quantified using LAS-1000plus/Image Gauge software (FUJIFILM, Tokyo, Japan).

In situ hybridization. For in situ hybridization, serial-cut 40-micrometer sections and non-radioactive digoxigenin-labeled cRNA probe against DARPP-32 (the dopamine- and cAMP-regulated phosphoprotein, Mr 32,000) were used as described previously [21].

Quantitative RT-PCR. Total RNA was extracted from the striatum using TRIZOL® Reagent (Invitrogen). Contaminating genomic DNA was removed with RQ1 RNase free DNase (Promega, Madison, WI) and 2 μg of total RNA was used for RT-PCR using Superscript™III First-Strand Synthesis System (Invitrogen). TaqMan PCR was performed using the TaqMan primer and probe sets as described [21]. Expression of GAPDH was estimated in each sample using the same methods for normalization.

Statistical analysis. Statistical significance was determined by Student's *t* test using StatView 5.0 (SAS Institute Inc., Cary, NC).

Results

Gene silencing by rAAV-shRNA

In vitro screening was used to identify the efficiency of mRNA ablation of shRNAs directed to EGFP and

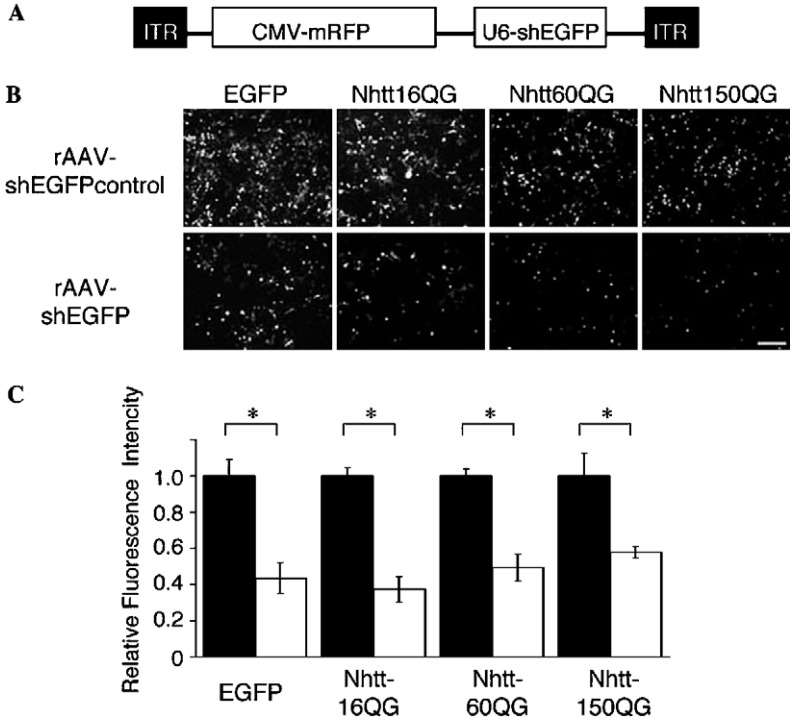

Fig. 1. rAAV-shEGFP reduced GFP expression in vitro. (A) AAV-shEGFP viral vector construct. ITR, inverted terminal repeat. CMV and U6 promoters were used for RFP and shEGFP. (B) Fluorescence photomicrographs of HEK-293 cells transfected with EGFP, Nhtt16QG, Nhtt60QG, and Nhtt150QG expression vectors and transduced with rAAV-shEGFP or rAAV-shEGFPcontrol, respectively. The photograph was taken after 48 h after viral transduction. Scale bar refers to all panels, 100 μm. (C) The relative level of GFP fluorescence intensity of rAAV-shEGFP transduced cells was compared to that of shEGFPcontrol transduced cells. The relative level of GFP fluorescence intensity of rAAV-shEGFPcontrol transduced cells (black bars); rAAV-shEGFP transduced cells (white bars). Values are given as means ± SEM ($n = 5$). $^{*}p < 0.001$.

EGFP-fused truncated htt-polyQ. EGFP-fused truncated htt-190Q is identical to the pathogenic transgene present in the HD190QG mouse [21]. The gene silencing function of 10 candidate shRNA sequences targeting EGFP was evaluated by the EGFP expression of co-transfected Neuro2A cells with shRNA and EGFP (data not shown). An shRNA targeting EGFP sequence 5′-GCAAGCTG ACCCTGAAGTTCAT-3′ (shEGFP) successfully reduced EGFP and EGFP-fused truncated htt expression significantly. Another shRNA targeting EGFP sequence 5′-GT TCATCTGCACCACCGGCTT-3′ had no gene silencing effect and was therefore used as a control (shEGFPcontrol). We next constructed an AAV-based vector (Fig. 1A). To test whether rAAV-mediated delivery of shEGFP could silence gene expression from EGFP or EGFP-fused truncated htt-polyQ, HEK293 cells were first transfected with EGFP or EGFP-fused truncated htt-polyQ expression vectors (EGFP, Nhtt16QG, Nhtt60QG, and Nhtt150QG, respectively), and subsequently transduced with rAAV2-shEGFP or rAAV2-shEGFPcontrol. shEGFP, but not shEGFPcontrol, significantly decreased GFP fluorescence intensity (Fig. 1B). The GFP intensity levels of shEGFP compared to those of shEGFPcontrol transduced cells were 0.43 ± 0.014, 0.37 ± 0.033, 0.50 ± 0.032, and 0.58 ± 0.027 (mean ± SEM, $n = 5$), in EGFP, Nhtt16QG, Nhtt60QG, and Nhtt150QG, respectively (Fig. 1C).

Expression and effect of shRNA in the mouse brain

rAAV5-shEGFP was injected into one side of the striatum and the same amount of buffer was injected into the other side of the striatum at 12 weeks old. The treated mice were sacrificed at 24 weeks old and serial-cut 40-micrometer sections were observed with laser-scanning imaging system. RFP fluorescence was expressed in the rAAV5-shEGFPinjected region and could show the infected cells (Fig. 2A). GFP fluorescence intensity was preferentially detected in the striatum, whereas the signal was decreased in the RFP-positive area. Further analysis at a higher magnification revealed that GFP fluorescent aggregates were absent in the RFP-positive neuronal cells up to three months after transduction of shEGFP in the striatum (Fig. 2B). In contrast, aggregates were abundantly observed in the contralateral side of the striatum. RFP expression was detected in the striatum as well as the cortex, lateral globus pallidus, hippocampus, and substantia nigra. However, reduction of GFP-positive aggregates was preferentially observed in the striatum, cortex, and hippocampus (data not shown).

Reduction of aggregate formation by shEGFP

Immunohistochemistry was performed using antibodies against GFP, htt, and ubiquitin. GFP and htt antibodies

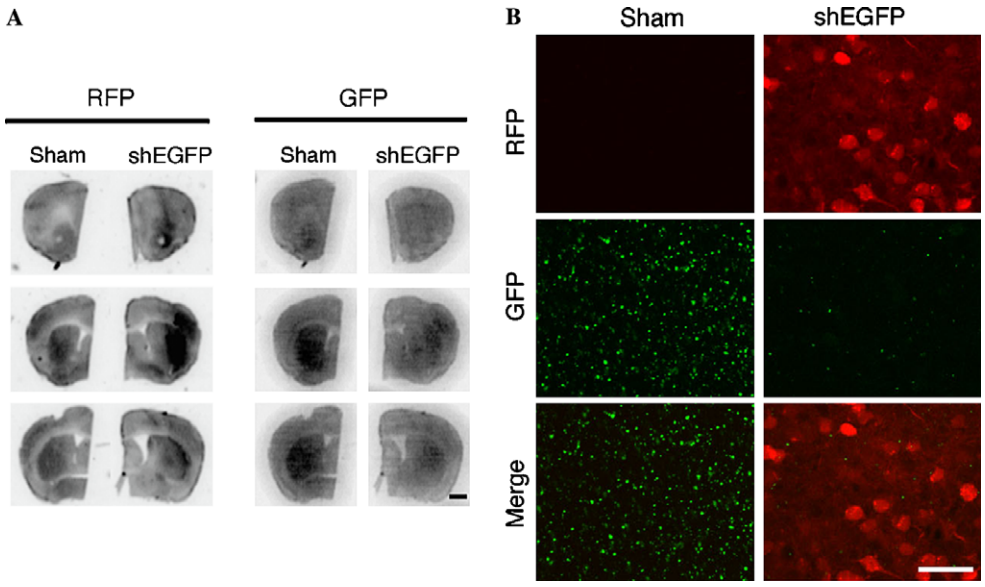

Fig. 2. rAAV-shEGFP transduction in the mouse brain decreases EGFP-positive aggregates (direct observation of EGFP fluorescence). (A) A montage of rostral-to-caudal coronal sections illustrates the extent of expression of RFP and EGFP in the brain. Three microliters of buffer was injected into striatum; sham, and rAAV-shEGFP was simultaneously injected into the contralateral side; shEGFP. Dark areas show fluorescent signal. Scale bar is 1 mm and refers to all panels. (B) EGFP fluorescence of the shEGFP-transduced striatum in high magnification. EGFP fluorescence was directly observed, while RFP was detected by anti-RFP because of the weak fluorescence after fixation. Scale bar is 20 μm and refers to all panels.

detect nuclear aggregates as well as cytoplasmic aggregates, and ubiquitin antibody detects large nuclear aggregates in HD190QG and R6/2 HD transgenic mice [10,21,25]. Reduction of aggregates is one of the indicators for the improvement of pathology in the HD mouse model [9,10,17,19]. In the HD190QG transgenic mouse, aggregate formation was first observed in the striatum at 4 weeks of age. Then, tremor, ataxia, and involuntary movements were observed at 6 weeks [21]. The shRNA was delivered to the striatum in 12 weeks old HD190QG mice to investigate the RNAi effects on disease pathology. At 24 weeks, mice brains were prepared for histological study. Immunohistochemistry was performed using antibodies against GFP, htt, and ubiquitin (Fig. 3A). The number of aggre-

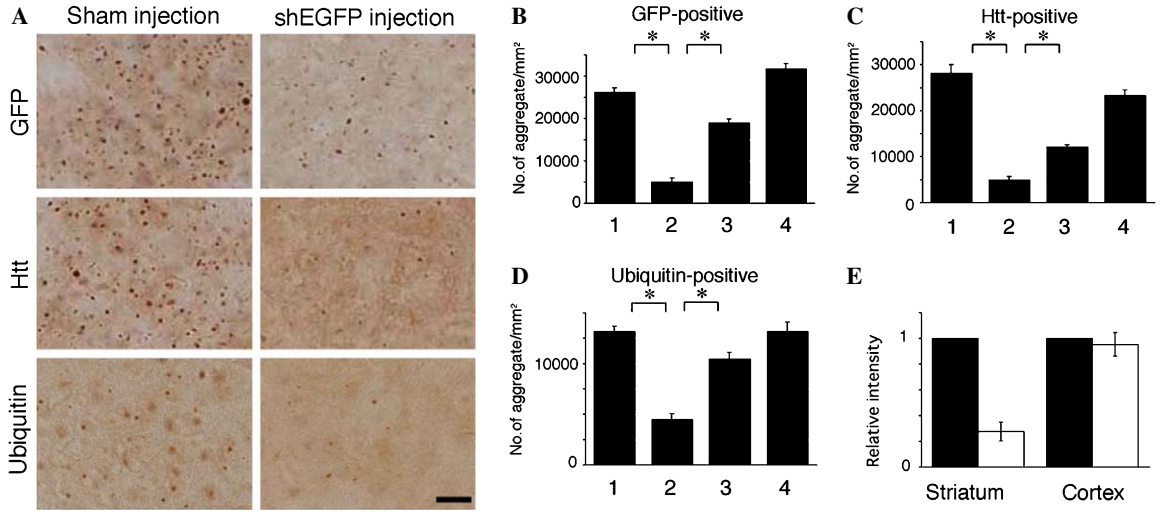

Fig. 3. shEGFP decreased antibody-positive aggregates and ameliorated aggregation pathology. (A) Representative images show GFP-, htt-, and ubiquitin-positive aggregates in the sham-injected or shEGFP-transduced striatum. Scale bar is 20 μm and refers to all panels. (B–D) Number of aggregates in the striatum is shown. rAAV-shEGFP was injected into the striatum at 12 weeks old and analyzed at 24 weeks old. The bars indicate aggregate number in the sham-injected striatum at 24 weeks old (1), shEGFP-transduced striatum at 24 weeks old (2), non-treated 12 weeks old HD190QG striatum, at the time point of shRNA transduction (3), and non-treated 24 weeks old HD190QG, as non-treatment control (4). The graphs show the number of GFP-positive aggregates (B), htt-positive aggregates (C), and ubiquitin-positive aggregates (D). Data are shown as average ± SEM (Y axis indicates the number of aggregates/mm^2. Sham-injected, shEGFP-transduced, and 12 weeks old control striatum; $n = 3$, 24 weeks old control striatum; $n = 4$). $^*p < 0.0001$. (E) Quantitative analysis of filter trap assay indicates relative amount of insoluble protein in the treated striatum. The relative fluorescence levels of sham-injected side (black) and shEGFP-transduced side (white) are shown as the average ± SEM ($n = 4$). $^*p < 0.0001$.

gates in the shEGFP-transduced striatum was much reduced than that in sham-injected striatum. The number of GFP-positive aggregates in shEGFP-transduced striatum was decreased to 19.4% of GFP-positive aggregates in sham injection striatum (Fig. 3B, bars 1 and 2). The number of htt-positive aggregates in shEGFP-transduced striatum was reduced to 17.7% of sham injection (Fig. 3C, bars 1 and 2), and the number of ubiquitin-positive aggregates in shEGFP-transduced striatum was reduced to 34.1% of sham injection (Fig. 3D, bars 1 and 2).

Furthermore, the number of aggregates in shEGFP-transduced striatum was significantly less than the number of aggregates formed in the striatum at the same age of shEGFP-transduction (Figs. 3B–D, bars 2 and 3). In this study, shEGFP-transduction was performed at 12 weeks old. The number of aggregate in shEGFP-transduced striatum at 24 weeks old was compared to that in 12 weeks old transgenic mice. The number of GFP-positive aggregates in shEGFP-transduced striatum was decreased to 26.8% of GFP-positive aggregates in 12 weeks old transgenic mice striatum (Fig. 3B, bars 2 and 3). The number of htt-positive aggregates in shEGFP-transduced striatum was reduced to 41.1% of 12 weeks old transgenic mice striatum (Fig. 3C, bars 2 and 3), and the number of ubiquitin-positive aggregates in shEGFP-transduced striatum was reduced to 42.9% of 12 weeks old transgenic mice striatum (Fig. 3D, bars 2 and 3). These results suggest that shEGFP was effective not only for inhibition of aggregation formation but also for clearance of aggregates that already existed in the nucleus and cytoplasm. The number of aggregates in the sham injection site was similar to that in the 24 weeks old transgenic mouse (Figs. 3B–D, bars 1 and 4). This result certifies that the injection procedure did not affect aggregation formation in the striatum. The number of aggregates was also not affected by rAAV-shEGFPcontrol transduction (data not shown).

We further investigated the effect of shEGFP on the accumulation of insoluble protein in the brain. In the HD190QG mouse brain, insoluble proteins including intra- and extra-nuclear aggregates increased in an age-dependent manner [21]. Filter trap assays revealed that insoluble protein accumulation was significantly suppressed in the shEGFP-transduced region compared to that in the sham-treated striatum, whereas it was not changed in the cortex. The reduction was 73% in the striatum and 5% in the cortex (Fig. 3E). Similar results were also obtained using htt antibody (data not shown).

Restoration of DARPP-32 expression by shRNA

To investigate the effect of shEGFP on striatal-specific transcripts, we first performed in situ hybridization using DARPP-32 probe, because DARPP-32 is known to be down-regulated in HD mouse [21,26]. We found the tendency of restored expression of DARPP-32 (Fig. 4A). Thus, we carried out the quantitative TaqMan RT-PCR analysis and confirmed that DARPP-32 and enkephalin mRNA expression was higher in the shEGFP-transduced striatum than the sham-injected side (Fig. 4B), suggesting that those gene expressions were partially restored.

Discussion

In this study, we demonstrated that neuropathological abnormalities associated with HD, such as insoluble protein accumulation and down-regulation of DARPP-32 expression, were successfully ameliorated by RNAi transduction. Following shRNA transduction, the number of neuronal aggregates in the striatum detected by ubiquitin antibody was reduced to 34.1% of that in the sham-treated striatum. Importantly, the number of aggregates in the shEGFP-transduced striatum was less than that in the striatum at the same time point of RNAi transduction.

Various treatments have shown an improvement of HD-associated abnormalities including pathological and behavioral deficits in a mouse model of HD [9,10,27–30]. Most treatments targeted downstream and possibly indirect effect of disease allele of htt, resulting in the delayed disease progression. Silencing of mutant gene expression was demonstrated using a conditional mouse model of HD [20]. Inhibition of mutant gene expression provides a direct approach to treat neurodegenerative diseases caused by toxic gain of function. RNAi is promising as a powerful tool for targeting gene knockdown. The silencing effect of synthesized siRNA injection was sustained more than 14 days in the newborn mouse brain to delay onset and prolong the life span of R6/2 [19]. In contrast, vector-based RNAi stably persisted more than 2–5 months after transduction, resulting in the improvement of motor dysfunction and neuropathological abnormalities [17,18]. AAV5 is efficient to transduce neuronal cells in the mouse brain [17,31,32], and shRNA expression by U6 promoter has been reported in mouse striatum [17]. Here we showed a drastic improvement of HD pathology in the mouse brain by rAAV5-mediated delivery of shRNA even the transduction was performed after the pathology appeared.

RNAi-mediated strategy has been performed as a pre-symptomatic treatment in the previous studies. We investigated whether RNAi treatment is functional on the pathology in the HD model after onset of disease. Gene silencing effects were observed at 2 weeks after virus injection in the symptomatic brain (data not shown), and the effect lasted for more than 3 months. Aggregate formation was effectively inhibited by shRNA transduction and the number of aggregates was decreased significantly compared with that in animals at the age of transduction. This result suggests that AAV-mediated delivery of shRNA could realize stable acquired gene knockdown in the transgenic mouse, and aggregate pathology was ameliorated as reported previously [20].

Expression of mutant htt leads to a decreased level of a subset of striatal-specific mRNAs of the HD190QG, R6/2, and R6/1 mouse [18,21,26]. DARPP-32, which is predominantly expressed in striatum, was down-regulated by 50%

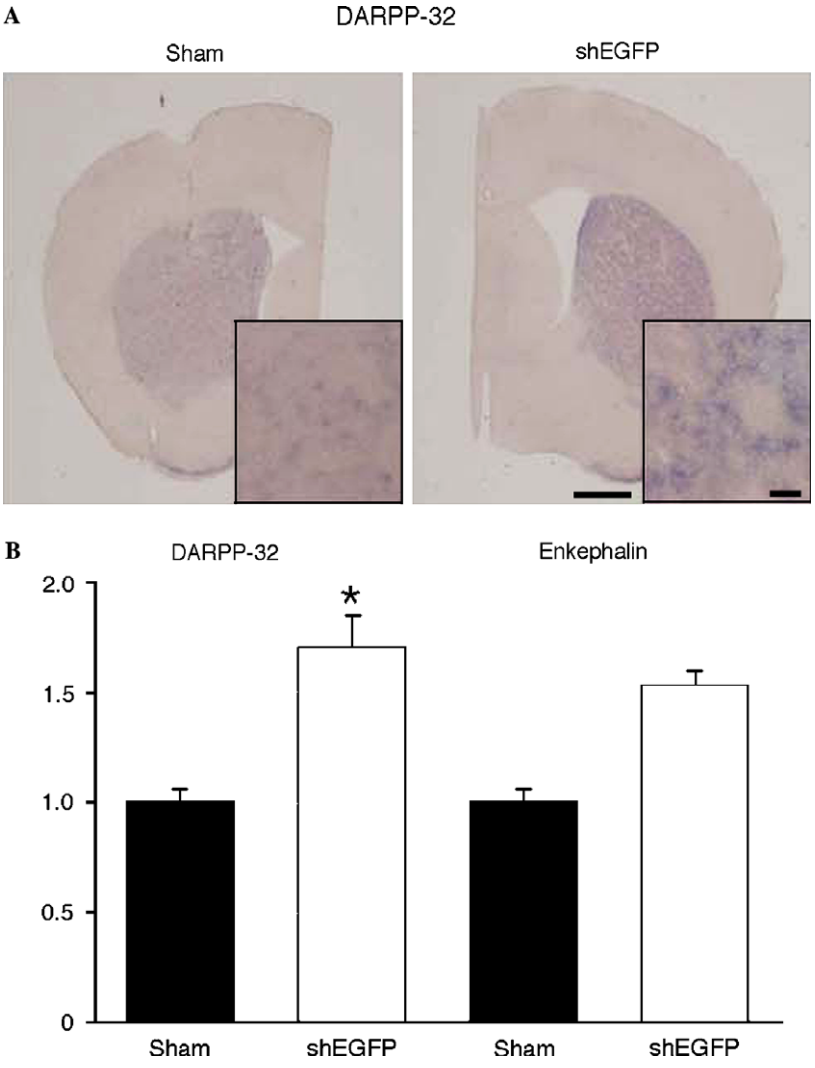

Fig. 4. shRNA restored DARPP-32 and enkephalin expression. (A) In situ hybridization of DARPP-32 at 24 weeks old after rAAV-shEGFP injection into the striatum at 9-week-old. Scale bar shows 1 mm. Higher magnification images of striatum are shown in inset, respectively, and scale bar is 20 μm. (B) DARPP-32 and enkephalin mRNA expression in striatum was determined by TaqMan RT-PCR analysis at 24 weeks after rAAV-shEGFP injection into the striatum performed at 12 weeks old. The expression levels of mRNA were normalized by that of GAPDH. DARPP-32 showed a significant increase in the shEGFP-injected side and enkephalin showed not significant but the tendency to restore. The values are given as means ± SEM ($n = 3$). $^{*}p < 0.05$.

in the 8-week-old HD190QG mouse compared with wild-type [21]. Here, we showed the restoration of DARPP-32 expression. Although the pathology was improved as shown in this report, we could not observe apparent improvement of the symptom or life span in this experiment. This is partly due to the injection was performed only in the one side to confirm the amelioration of the pathology and due to the injection time point, which restricted the full restoration of the function. Further study to determine the critical time of viral transduction for the functional recovery is necessary.

In this study, we used shRNA against EGFP for HD190QG mouse to suppress only the transgene. This shEGFP is designed to modulate mutant htt expression in our animal model but not applicable to the clinical investigation of human HD gene therapy. Although either siRNA or shRNA against htt was produced and investigated previously [17–19], this siRNA sequence reduced not only mutant htt but also wild-type htt simultaneously. Since wild-type htt is essential to embryogenesis, the complete loss of wild-type htt results in embryonic lethality and reduction of wild-type htt leads to behavioral abnormalities and neuronal loss [33]. In fact, loss of wild-type htt in YAC128 mice induced motor dysfunction and survival was worse compared with YAC128 mice expressing wild-type htt [33]. For these reasons, it is required to design a siRNA sequence, which selectively silences mutant htt but not wild-type htt. When a technology is developed to solve this issue, RNAi-based therapy would be practical for pre- and post-symptomatic treatment strategy for HD therapy [15,24].

In summary, we showed that RNAi dramatically improved HD-associated pathological abnormalities in a mouse model of HD, although the treatment was carried out after onset of symptom. Our data suggested that reduction of mutant gene expression by RNAi would be

promising to attenuate disease progression in post-symptomatic neurodegenerative disorders.

Acknowledgments

The authors thank Dr. John A. Chiorini for providing pAAV5-RNL and pAAV5-RepCap (identical to 5RepCapB) and Avigen, Inc. (Alameda, CA) for providing pAAV-LacZ, pHLP19, and pAdeno. We also thank Drs. Nobuhisa Iwata, Takaomi Saido, Mayumi Okada, and Ms. Miyoko Mitsu for their technical supports and Drs. Joanna Doumanis and Hong-Kit Wong for their critical readings. This work was supported in part by grants from Grants-in-Aid for Scientific Research on Priority Areas 17025044 from The Ministry of Education, Culture, Sports, Science and Technology (MEXT) and the Ministry of Health, Labour and Welfare.

References

[1] J.F. Gusella, M.E. MacDonald, Molecular genetics: unmasking polyglutamine triggers in neurodegenerative disease, Nat. Rev. Neurosci. 1 (2000) 109–115.
[2] A.W. Dunah, H. Jeong, A. Griffin, Y.M. Kim, D.G. Standaert, S.M. Hersch, M.M. Mouradian, A.B. Young, N. Tanese, D. Krainc, Sp1 and TAFII130 transcriptional activity disrupted in early Huntington's disease, Science 296 (2002) 2238–2243.
[3] C.J. Cummings, M.A. Mancini, B. Antalffy, D.B. DeFranco, H.T. Orr, H.Y. Zoghbi, Chaperone suppression of aggregation and altered subcellular proteasome localization imply protein misfolding in SCA1, Nat. Genet. 19 (1998) 148–154.
[4] N.R. Jana, M. Tanaka, G. Wang, N. Nukina, Polyglutamine length-dependent interaction of Hsp40 and Hsp70 family chaperones with truncated N-terminal huntingtin: their role in suppression of aggregation and cellular toxicity, Hum. Mol. Genet. 9 (2000) 2009–2018.
[5] U. Nagaoka, K. Kim, N.R. Jana, H. Doi, M. Maruyama, K. Mitsui, F. Oyama, N. Nukina, Increased expression of p62 in expanded polyglutamine-expressing cells and its association with polyglutamine inclusions, J. Neurochem. 91 (2004) 57–68.
[6] H. Doi, K. Mitsui, M. Kurosawa, Y. Machida, Y. Kuroiwa, N. Nukina, Identification of ubiquitin-interacting proteins in purified polyglutamine aggregates, FEBS Lett. 571 (2004) 171–176.
[7] N.F. Bence, R.M. Sampat, R.R. Kopito, Impairment of the ubiquitin-proteasome system by protein aggregation, Science 292 (2001) 1552–1555.
[8] A.V. Panov, C.A. Gutekunst, B.R. Leavitt, M.R. Hayden, J.R. Burke, W.J. Strittmatter, J.T. Greenamyre, Early mitochondrial calcium defects in Huntington's disease are a direct effect of polyglutamines, Nat. Neurosci. 5 (2002) 731–736.
[9] I. Sanchez, C. Mahlke, J. Yuan, Pivotal role of oligomerization in expanded polyglutamine neurodegenerative disorders, Nature 421 (2003) 373–379.
[10] M. Tanaka, Y. Machida, S. Niu, T. Ikeda, N.R. Jana, H. Doi, M. Kurosawa, M. Nekooki, N. Nukina, Trehalose alleviates polyglutamine-mediated pathology in a mouse model of Huntington disease, Nat. Med. 10 (2004) 148–154.
[11] S.M. Elbashir, J. Harborth, W. Lendeckel, A. Yalcin, K. Weber, T. Tuschl, Duplexes of 21-nucleotide RNAs mediate RNA interference in cultured mammalian cells, Nature 411 (2001) 494–498.
[12] J.Y. Yu, S.L. DeRuiter, D.L. Turner, RNA interference by expression of short-interfering RNAs and hairpin RNAs in mammalian cells, Proc. Natl. Acad. Sci. USA 99 (2002) 6047–6052.
[13] A.P. McCaffrey, M.A. Kay, A story of mice and men, Gene Ther. 9 (2002) 1563.
[14] H. Hasuwa, K. Kaseda, T. Einarsdottir, M. Okabe, Small interfering RNA and gene silencing in transgenic mice and rats, FEBS Lett. 532 (2002) 227–230.
[15] G.S. Ralph, P.A. Radcliffe, D.M. Day, J.M. Carthy, M.A. Leroux, D.C. Lee, L.F. Wong, L.G. Bilsland, L. Greensmith, S.M. Kingsman, K.A. Mitrophanous, N.D. Mazarakis, M. Azzouz, Silencing mutant SOD1 using RNAi protects against neurodegeneration and extends survival in an ALS model, Nat. Med. 11 (2005) 429–433.
[16] H. Xia, Q. Mao, S.L. Eliason, S.Q. Harper, I.H. Martins, H.T. Orr, H.L. Paulson, L. Yang, R.M. Kotin, B.L. Davidson, RNAi suppresses polyglutamine-induced neurodegeneration in a model of spinocerebellar ataxia, Nat. Med. 10 (2004) 816–820.
[17] S.Q. Harper, P.D. Staber, X. He, S.L. Eliason, I.H. Martins, Q. Mao, L. Yang, R.M. Kotin, H.L. Paulson, B.L. Davidson, RNA interference improves motor and neuropathological abnormalities in a Huntington's disease mouse model, Proc. Natl. Acad. Sci. USA 102 (2005) 5820–5825.
[18] E. Rodriguez-Lebron, E.M. Denovan-Wright, K. Nash, A.S. Lewin, R.J. Mandel, Intrastriatal rAAV-mediated delivery of anti-huntingtin shRNAs induces partial reversal of disease progression in R6/1 Huntington's disease transgenic mice, Mol. Ther. 12 (2005) 618–633.
[19] Y.L. Wang, W. Liu, E. Wada, M. Murata, K. Wada, I. Kanazawa, Clinico-pathological rescue of a model mouse of Huntington's disease by siRNA, Neurosci. Res. (2005).
[20] A. Yamamoto, J.J. Lucas, R. Hen, Reversal of neuropathology and motor dysfunction in a conditional model of Huntington's disease, Cell 101 (2000) 57–66.
[21] S. Kotliarova, N.R. Jana, N. Sakamoto, M. Kurosawa, H. Miyazaki, M. Nekooki, H. Doi, Y. Machida, H.K. Wong, T. Suzuki, C. Uchikawa, Y. Kotliarov, K. Uchida, Y. Nagao, U. Nagaoka, A. Tamaoka, K. Oyanagi, F. Oyama, N. Nukina, Decreased expression of hypothalamic neuropeptides in Huntington disease transgenic mice with expanded polyglutamine-EGFP fluorescent aggregates, J. Neurochem. 93 (2005) 641–653.
[22] R.E. Campbell, O. Tour, A.E. Palmer, P.A. Steinbach, G.S. Baird, D.A. Zacharias, R.Y. Tsien, A monomeric red fluorescent protein, Proc. Natl. Acad. Sci. USA 99 (2002) 7877–7882.
[23] T. Okada, K. Shimazaki, T. Nomoto, T. Matsushita, H. Mizukami, M. Urabe, Y. Hanazono, A. Kume, K. Tobita, K. Ozawa, N. Kawai, Adeno-associated viral vector-mediated gene therapy of ischemia-induced neuronal death, Methods Enzymol. 346 (2002) 378–393.
[24] T. Okada, T. Nomoto, T. Yoshioka, M. Nonaka-Sarukawa, T. Ito, T. Ogura, M. Iwata-Okada, R. Uchibori, K. Shimazaki, H. Mizukami, A. Kume, K. Ozawa, Large-scale production of recombinant viruses by use of a large culture vessel with active gassing, Hum. Gene Ther. 16 (2005) 1212–1218.
[25] S.W. Davies, M. Turmaine, B.A. Cozens, M. DiFiglia, A.H. Sharp, C.A. Ross, E. Scherzinger, E.E. Wanker, L. Mangiarini, G.P. Bates, Formation of neuronal intranuclear inclusions underlies the neurological dysfunction in mice transgenic for the HD mutation, Cell 90 (1997) 537–548.
[26] R. Luthi-Carter, A. Strand, N.L. Peters, S.M. Solano, Z.R. Hollingsworth, A.S. Menon, A.S. Frey, B.S. Spektor, E.B. Penney, G. Schilling, C.A. Ross, D.R. Borchelt, S.J. Tapscott, A.B. Young, J.H. Cha, J.M. Olson, Decreased expression of striatal signaling genes in a mouse model of Huntington's disease, Hum. Mol. Genet. 9 (2000) 1259–1271.
[27] R.J. Ferrante, J.K. Kubilus, J. Lee, H. Ryu, A. Beesen, B. Zucker, K. Smith, N.W. Kowall, R.R. Ratan, R. Luthi-Carter, S.M. Hersch, Histone deacetylase inhibition by sodium butyrate chemotherapy ameliorates the neurodegenerative phenotype in Huntington's disease mice, J. Neurosci. 23 (2003) 9418–9427.
[28] R.J. Ferrante, O.A. Andreassen, B.G. Jenkins, A. Dedeoglu, S. Kuemmerle, J.K. Kubilus, R. Kaddurah-Daouk, S.M. Hersch, M.F.

Beal, Neuroprotective effects of creatine in a transgenic mouse model of Huntington's disease, J. Neurosci. 20 (2000) 4389–4397.

[29] M. Chen, V.O. Ona, M. Li, R.J. Ferrante, K.B. Fink, S. Zhu, J. Bian, L. Guo, L.A. Farrell, S.M. Hersch, W. Hobbs, J.P. Vonsattel, J.H. Cha, R.M. Friedlander, Minocycline inhibits caspase-1 and caspase-3 expression and delays mortality in a transgenic mouse model of Huntington disease, Nat. Med. 6 (2000) 797–801.

[30] M.V. Karpuj, M.W. Becher, J.E. Springer, D. Chabas, S. Youssef, R. Pedotti, D. Mitchell, L. Steinman, Prolonged survival and decreased abnormal movements in transgenic model of Huntington disease, with administration of the transglutaminase inhibitor cystamine, Nat. Med. 8 (2002) 143–149.

[31] C. Burger, O.S. Gorbatyuk, M.J. Velardo, C.S. Peden, P. Williams, S. Zolotukhin, P.J. Reier, R.J. Mandel, N. Muzyczka, Recombinant AAV viral vectors pseudotyped with viral capsids from serotypes 1, 2, 5 display differential efficiency and cell tropism after delivery to different regions of the central nervous system, Mol. Ther. 10 (2004) 302–317.

[32] M.Y. Mastakov, K. Baer, R.M. Kotin, M.J. During, Recombinant adeno-associated virus serotypes 2- and 5-mediated gene transfer in the mammalian brain: quantitative analysis of heparin co-infusion, Mol. Ther. 5 (2002) 371–380.

[33] J.M. Van Raamsdonk, J. Pearson, D.A. Rogers, N. Bissada, A.W. Vogl, M.R. Hayden, B.R. Leavitt, Loss of wild-type huntingtin influences motor dysfunction and survival in the YAC128 mouse model of Huntington disease, Hum. Mol. Genet. 14 (2005) 1379–1392.